

CONF-771029--15

# Lawrence Livermore Laboratory

CHARGED PARTICLE FUSION TARGETS

R.O. BANGERTER AND D.J. MEEKER

November 9, 1977

This paper was prepared for presentation at the 2nd International Topical Conference on High Power Electron and Ion Beam Research and Technology to be held in Ithaca, New York, October 3-5, 1977.

This is a preprint of a paper intended for publication in a journal or proceedings. Since changes may be made before publication, this preprint is made available with the understanding that it will not be cited or reproduced without the permission of the author.



## CHARGED PARTICLE FUSION TARGETS\*

R. O. Bangerter and D. J. Meeker

University of California, Lawrence Livermore Laboratory  
Livermore, California

### Abstract

In this paper we review the power, voltage, energy and other requirements of electron and ion beam fusion targets. We discuss single shell, multiple shell and magnetically insulated target designs. Questions of stability are also considered. In particular, we show that ion beam targets are stabilized by an energy spread in the ion beam.

### Introduction

In this paper we review the status of charged particle fusion target design at the time of the 1st International Conference on Electron Beam Research and Technology and describe some of the innovations and progress of the intervening two years.

Targets having gain (thermonuclear yield/input energy)  $\leq 1$  are interesting from a scientific point of view and considerable progress has been made in the design of these targets. However, ultimately targets having gain considerably greater than 1 are needed. In order to limit the scope of this paper we discuss only targets having gain  $\geq 1$ .

---

\*Research performed under the auspices of the U.S. Department of Energy under contract No. W7405-ENG-48.

## Electron Beam Targets

Two of the targets discussed at the last conference<sup>1,2</sup> are shown in Fig. 1 and 2.

In one-dimensional computer simulations, the target in Fig. 1 achieves gain  $\approx 1$  at a peak input power of 360 TW.<sup>3</sup> A similar target with a carbon ablator gives gain = 1 at an input power of 225 TW.<sup>4</sup> The two-shell design of Fig. 2 achieves gain  $\approx 1$  at a peak input power of 250 TW.

Relatively little progress has been made in improving these electrons driven targets during the last two years. Calculations at Sandia Laboratories on time-varying voltage pulses<sup>5</sup> have not been very encouraging. Some calculations have been performed at Livermore on targets similar to that shown in Fig. 1 but having larger yield. In particular, the target shown in Fig. 1 gives a yield of 242 MJ with a DT fuel mass of 880  $\mu\text{g}$ . The required input power is 1200 TW. The input energy is 6.6 MJ and the gain is 24.

## Ion Beam Targets

Two years ago the ion beam targets shown in Fig. 3 and 4 were reported.<sup>1,2</sup> A newer target design is shown in Fig. 5.<sup>6</sup> The principal feature of this target is the high Z, high density tamper surrounding the low Z, low density pusher. Low Z materials are more effective in stopping ions than high Z materials. This is illustrated in Fig. 6. The enhanced deposition in the low Z material creates a tamped explosion that efficiently drives the fuel inward. The characteristics of this target are given in Table I. The chief advantage of this target is that it gives high gain ( $\sim 100$ ) at relatively modest input power and energy. High target gain is expected to significantly reduce the cost of an inertial confinement fusion power plant. The chief disadvantage of this

3  
target is the requirement of rather precise pulse shaping.

#### Magnetically Insulated Targets

An approach to target design that has been extensively studied since the 1975 Conference is the addition of a magnetic field to the fuel region. This is illustrated in Fig. 7. The purpose of the magnetic field is two-fold. If the fuel is at a sufficiently low density, the magnetic field can inhibit thermal conduction from the DT to the surrounding pusher wall. This allows one to use preheat in the DT and then do a nearly adiabatic compression of the fuel to reach ignition conditions. A second advantage occurs at maximum compression. If the initial magnetic field is sufficiently large, the resulting compressed field can trap the alpha particles produced by the DT fusion reactions thereby heating the burning plasma even further. The net result is a target design that should allow one to reduce the input requirement of the driving source.

Results of one class of these targets designed for 10 MeV protons is shown in Table II. They are characterized by relatively low input powers and, for the larger sizes, no pulse shaping requirement. Thus the advantage of low power appears to be possible.

There are disadvantages, however. The magnitude of magnetic field required is quite large if thermal conduction is to be limited. Several methods of producing this field are shown in Fig. 8 but all fall short of producing the large fields needed by these targets.

Furthermore, even with magnetic fields the fuel density must be low to maintain a large  $\alpha$ . This low fuel density forces one to accept low gain or to face the difficulty of fabricating and propagating the burn into a dense fuel layer surrounding the low density core.

For high gain targets questions of fuel cleanliness, implosion symmetry, fluid instability and target fabrication must be addressed.

In spite of these difficulties, the appeal of low power sources producing significant gain continues to be of interest and we shall investigate this approach further.

#### Ion Beam Target Stability

The consequences of Rayleigh-Taylor instability were discussed at the last conference.<sup>1,2</sup> The growth rate for this instability is given by  $\gamma = \sqrt{ka} \alpha$  where  $\alpha$  is the Atwood number,  $k$  is the wave number and  $a$  is the acceleration perpendicular to the unstable interface. If the unstable interface is replaced by a region in which the density varies exponentially with scale length  $L = 1/\beta$  one must make the replacement  $k \rightarrow \frac{k\beta}{k+\beta}$ .<sup>7</sup> When  $\beta \leq k$  this effect becomes important and results in considerable stabilization. Because of multiple scattering and bremsstrahlung, 1 MeV electrons have a deposition profile that falls off very gradually at the end of the range. Such an extended deposition profile results in minimal sensitivity to fluid instabilities, but also considerable preheat and low thermonuclear gains. Ions, with a sharp cutoff at the end of their range, result in more efficient, lower power implosions but greatly increased sensitivity to fluid instability. However, putting an energy spread on the ion beam will spread out the deposition at the end of the range. By suitably choosing this spread in energy and adjusting shell thicknesses appropriately, one can still achieve a relatively efficient implosion but with greatly reduced sensitivity to fluid instability. Figure 9 shows the plots of  $dE/dx$  for an ion beam with an average energy of 10 MeV under various conditions. Curve A is the deposition profile for a monoenergetic beam focused radially onto a spherical target. Curve B is the profile for a

monochromatic beam but assumes a 10 eV transverse temperature at the source which spreads the beam to 1.66 mm FWHM at a distance of 1 m from the source. Hence, the beam is no longer radially focused. Curve C is the profile for a beam with an average energy of 10 MeV but with a gaussian spread in energies of 17.6% FWHM and a 10 eV transverse temperature at the source. These sources are applied to the target shown in Fig. 10. The target consists of a gold shell with a 2 mm inner radius and 1 mg of solid DT in a 100  $\mu$  thick inner layer. The gold shell varies in thickness from 0.21 mm for the radial deposition A to 0.23 mm for the deposition C.

For deposition A the required power is 500 TW while for deposition C the required power increased to 700 TW.

The higher power for case C occurs because the gold shell is thicker to accommodate the greater ion range and because the implosion is somewhat less efficient with the extended deposition profile.

Shown in Fig. 11 is a plot of the density scale length  $l$  as a function of time for the three deposition profiles. Plotted for reference is  $1/k$  versus time for  $l = 100$ . For the radial profile A, the scale length is much less than  $1/k$  while for C, the scale length exceeds  $1/k$ .

Note that a greater shell thickness also goes with a shallower density gradient as shown in Fig. 12. Some of the increase is due to the fact that the initial shell is thicker for case C.

The reduction in growth as one goes from A to C is evident from the dispersion relations given in Fig. 13. The curves are analytic relations and show  $\ln(\eta/\eta_0) = \int \gamma dt$  as a function of  $k$ . The quantities  $\eta_0$  and  $\eta$  are respectively the initial and final perturbation amplitude. The results are from LASNEX calculations. As a result of the modified

density gradient, case C easily survives with  $10.1 \text{ \AA}$  surface finish.

In conclusion, it should be possible to exploit density gradient modification to reduce the sensitivity to fluid instability of charged particle driven micro-fusion implosions.

For ion beams sources, the reduction is achieved by introducing an energy spread on the driving source. This may have important consequences for pulsed power technology.

#### References

1. E.J. Clauser and M.A. Sweeney, International Topical Conference on Electron Beam Research and Technology, Sandia Laboratories Report, SAND 76-5122, Vol I, 135 (February 1976).
2. J.D. Lindl and R.O. Bangerter, International Conference on Electron Beam Research and Technology, Sandia Laboratories Report, SAND 76-5122, Vol I, 37 (February 1976).
3. Calculations performed at Lawrence Livermore Laboratory using the IASNEX simulation code give a power requirement of 400 TW for this target.
4. M.A. Sweeney, Applied Physics Letters 29, 231 (1976).
5. Electron Beam Fusion Progress Report July through September 1976, Sandia Laboratories Report SAND 76-0711, 33 (May 1977).
6. R. Bangerter and D. Meeker, Lawrence Livermore Laboratory Report, UCRL-78474 (October 1976).
7. R. LeVieir, G. Iasher, F. Bjorklung, Lawrence Radiation Laboratory Report, UCRL-4459 (1955).

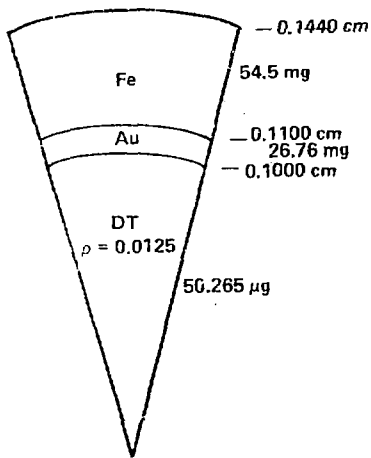


Fig. 1 - Single Shell Target Driven by 1 MeV Electrons

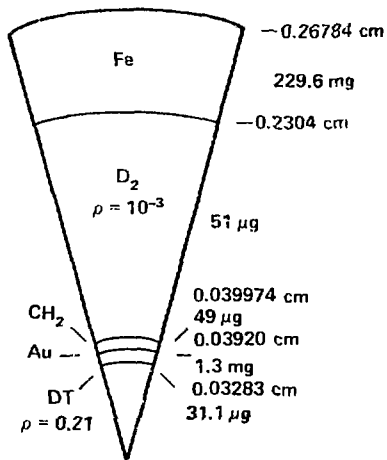


Fig. 2 - Double Shell Target Driven by 1 MeV Electrons

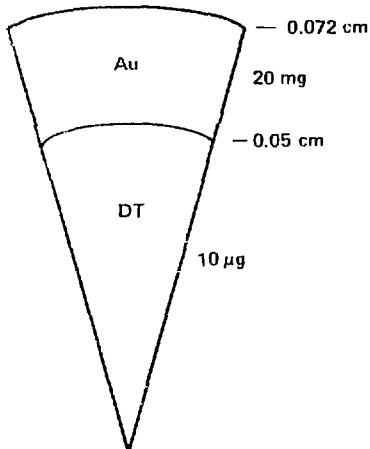


Fig. 3 - Single Shell Target Driven by 10 MeV Protons

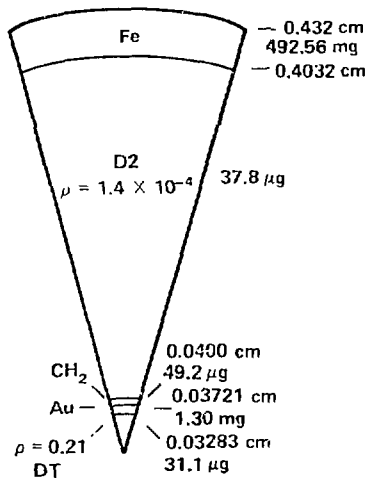


Fig. 4 - Double Shell Target Driven by 10 MeV Protons



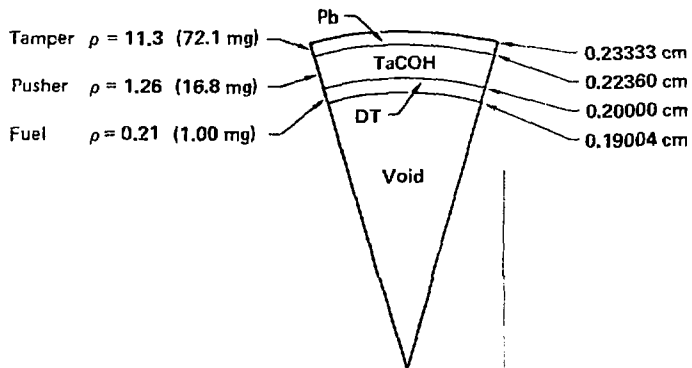


Fig. 5 - Ion Beam Fusion Target with Low Density Pusher.

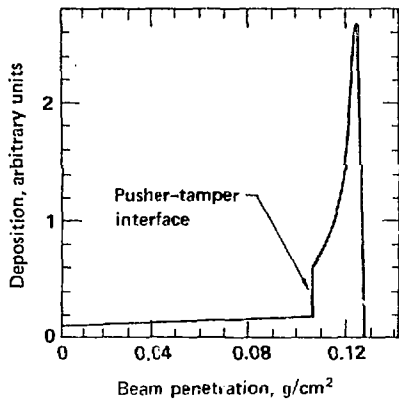


Fig. 6 - Deposition Profile For 6.5 MeV Protons Incident on Target.

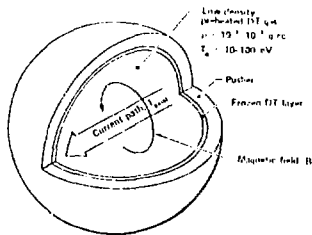


Fig. 7 - Magnetically Insulated Targets

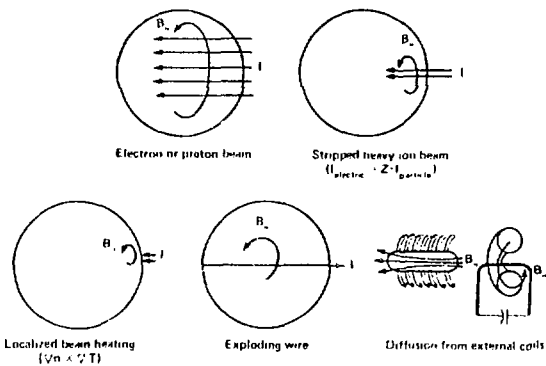


Fig. 8 - Various Methods of Obtaining Magnetic Fields

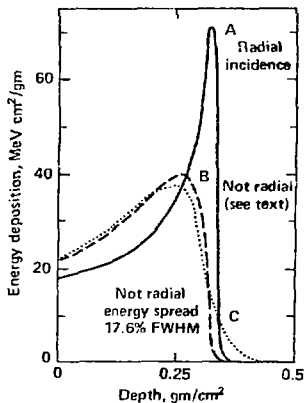


Fig. 9 - Energy Deposition of 10 MeV Protons in Gold at a Temperature of 200 eV and Density of 5 gm/cm<sup>3</sup>.

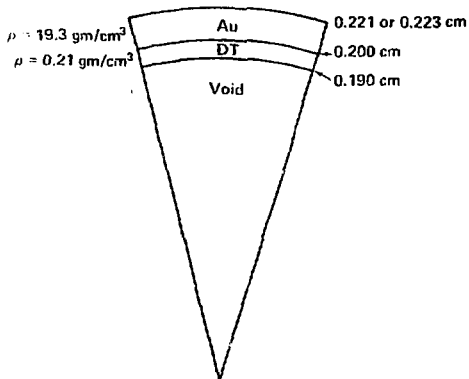


Fig. 10 - Target Used for Ion Beam, Density Gradient Stabilization Study.

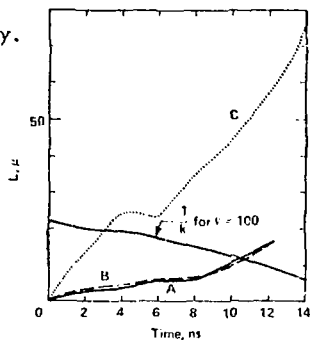


Fig. 11 - Density Scale Length as a Function of Time for Ion Beam Target.

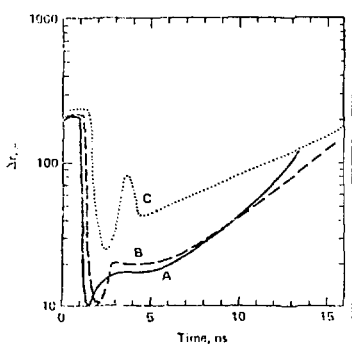


Fig. 12 - Shell Thickness as a Function of Time for 10 MeV Proton Target.

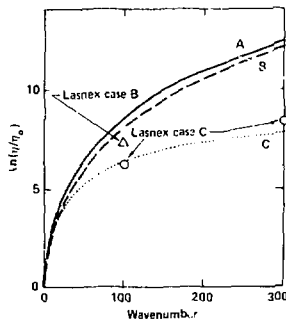


Fig. 13 - Number of e-Foldings as a Function of Wavenumber for Ion Beam Target.

Time, ns	Power, TW
0	1.6
10	1.6
14	16
17	240.0
20.5	240.0

Power varies linearly between values listed.

Input energy MJ	1.28
Yield, MJ	113.0
Gain	88.0

Table 1 - Properties of Ion Beam Target with Low Density Pusher

fuel radius	0.2 cm	0.1	0.05	0.025 cm
Input power	80TW/25ns	35TW/10ns	1TW/1.5ns 3TW/1.5-3ns 30TW/3.8-9ns	0.5TW/1.8ns 2TW/1.8-2.1ns 8TW/2.1-2.4ns 30TW/3.4-4.9ns
Input energy (MJ)	2.1	0.45	0.2	0.079
Yield (MJ)	189	15	0.67	0.087
Gain	84	34	3.4	1.1
Max. interface velocity (cm/ns)	12	11	14	14
Minimum fuel radius (cm)	0.011	0.0045	0.0019	0.0014
Compression ratio	5900	11,000	17,000	6,000
Max. fuel temperature (keV)	270	110	29	28
Max. fuel density (g/cc)	230	340	560	560
Max. fuel pressure (g/cm <sup>2</sup> )	0.42	0.5	0.28	0.11

Table 2 - Summary of Optimized Ion Driven Targets Employing Magnetic Fields